Geological Survey of Canada

CURRENT RESEARCH
2006-B1

Pore-size-distribution characteristics of Beaufort-Mackenzie Basin shale samples, Northwest Territories

S. Connell-Madore and T.J. Katsube

2006

Natural Resources Canada
Ressources naturelles Canada

Canada

CURRENT RESEARCH

ISSN 1701-4387
Catalogue No. M44-2006/B1E-PDF
ISBN 0-662-43612-1

A copy of this publication is also available for reference by depository libraries across Canada through access to the Depository Services Program's Web site at http://dsp-psd.pwgsc.gc.ca

A free digital download of this publication is available from GeoPub:
http://geopub.nrcan.gc.ca/index_e.php

Toll-free (Canada and U.S.A.): 1-888-252-4301

Critical reviewers
B. Medioli

Authors' addresses

S. Connell-Madore (sconnell@nrcan.gc.ca)
T.J. Katsube (jkatsube@nrcan.gc.ca)
GSC Northern Canada
Geological Survey of Canada
601 Booth Street
Ottawa, Ontario K1A 0E8

Publication approved by GSC Northern Canada

Original manuscript submitted: 2006-04-06
Final version approved for publication: 2006-04-07

Correction date:

Pore-size-distribution characteristics of Beaufort-Mackenzie Basin shale samples, Northwest Territories

S. Connell-Madore and T.J. Katsube

Connell-Madore, S. and Katsube, T.J., 2006: Pore-size-distribution characteristics of Beaufort-Mackenzie Basin shale samples; Geological Survey of Canada, Current Research 2006-B1, 13 p.

Abstract: Pore-size-distribution patterns for forty-one Beaufort-Mackenzie Basin shale samples have been examined for trends and similarities within four shale-compaction zones. These samples were collected over a depth range of 950 to 4860 m in nine wells. The main purpose of this study was to document trends related to depth and overpressure. This will form a database for pore-structure determination and seal-quality evaluation in future studies.

Results indicate a distinct change in pore-size-distribution patterns at a depth of approximately 2 km in all four zones, with little to no change specifically related to normal versus overpressured areas. The main difference in the pore-size distributions at this depth (2 km) occurs in the intermediate and micro pore sizes. At a depth of 2 km, the relationship between other parameters (e.g. total porosity, density) and depth also changes.

Résumé : La répartition de la taille des pores dans 41 échantillons de shale provenant du bassin de Beaufort-Mackenzie a été analysée afin d'établir des tendances et des similarités pour quatre zones de compaction du shale. Les échantillons ont été prélevés dans neuf puits, à des profondeurs allant de 950 à 4 860 m. Leur analyse visait principalement à relever des tendances liées à la profondeur et à la surpression, afin de produire une base de données qui servira, lors d'études ultérieures, à déterminer la structure de l'espace interstitiel et à évaluer les qualités d'étanchéité des sédiments.

Les résultats témoignent d'un changement distinct de répartition de la taille des pores à quelque 2 km de profondeur dans les quatre zones, alors que la différence de répartition de la taille des pores est minime, voire nulle, entre les zones de surpression et celles de pression normale. À 2 km de profondeur, la répartition de la taille des pores change surtout pour les pores de taille « intermédiaire » à « micro »; par ailleurs, la relation entre la profondeur et d'autres paramètres (p. ex. la porosité totale et la densité) change également à cette profondeur.

INTRODUCTION

With increased burial depth and compaction, shale units can evolve into effective seals that form barriers to the upward movement of fluids and hydrocarbons. At relatively shallow depths (up to 500 m below sea level), they can be the source of hazardous shallow waterflow (Katsube and Jonasson, 2002) and provide a seal for gas-hydrate accumulations (Katsube et al., 2004). At greater depths, shale can act as a caprock for conventional petroleum accumulations and contribute to the development of abnormal formation pressures (e.g. Huffman and Bowers, 2002). From a petrophysical viewpoint, these properties are mainly due to the pore-size distribution of the rocks, which always includes a <30 nm pore-size component (e.g. Katsube and Williamson, 1998; Katsube et al., 1999), their low (<10 to 21 m^2; Katsube and Connell, 1998) to relatively low (<10 to 19 m^2; Katsube and Connell, 1998) permeability (k), and their connecting pore structure (pore-space distribution between the storage pores).

Table 1. Identification of samples used in the study (*from* Katsube and Issler, 1993).

Sample	Well	True vertical depth (m)	Zone
B-AM-1	Amuligak (F-24)	4376.5	2
B-AM-2		4395.0	2
B-AM-3		4695.0	2
B-AR-1	Amerk (O-09)	1317.0	2
B-AR-2		1533.0	2
B-AR-3		1765.0	2
B-AR-4		3866.0	2
B-AR-5		4375.0	2
B-AR-6		4606.0	2
B-AR-7		4861.0	2
B-AK-1	Arluk (E-90)	3452.0	1
B-AK-2		3938.0	1
B-ML-1	Mallik (A-06)	1362.0	4
B-ML-2		3215.0	4
B-ML-3		3609.0	4
B-NR-1	Nerlerk (J-67)	3945.0	1
B-NR-2		3962.0	1
B-NR-3		4357.5	1
B-RE-1	Reindeer (D-27)	1458.0	4
B-RE-2		1469.0	4
B-RE-3		2022.0	4
B-RE-4		2092.0	4
B-RE-5		2099.0	4
B-RE-6		2213.0	4
B-RE-7		2389.0	4
B-RE-8		2421.0	4
B-RE-9		2551.0	4
B-RE-10		2725.0	4
B-RE-11		2923.0	4
B-RE-12		3153.0	4
B-RE-13		3481.0	4
B-RE-14		3628.0	4
B-TA-1	Taglu (C-42)	2881.0	3
B-TA-2	Taglu (F-43)	3247.0	3
B-TG(33)-1	Taglu (G-33)	952.0	3
B-TG(33)-2		1350.0	3
B-TG(33)-3		1640.0	3
B-TG(33)-4		2075.0	3
B-TG(33)-5		2459.0	3
B-TG(33)-6		2460.0	3
B-TG(33)-7		2533.0	3

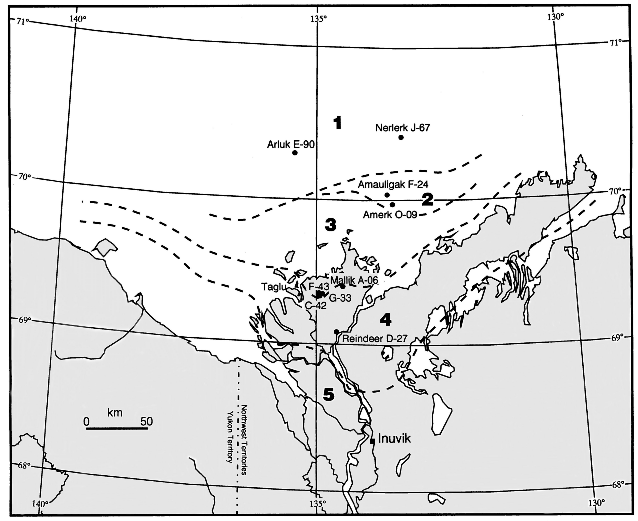

Figure 1. Location of the nine wells in the Beaufort-Mackenzie Basin, Northwest Territories, and the approximate boundaries of the five shale-compaction zones (Issler, 1992), which are shown by heavy dashed lines.

Data on pore-size distribution for 41 previously published shale samples from the Beaufort-Mackenzie Basin, Northwest Territories (Katsube and Issler, 1993) form a database for determining the pore-structure variables (Katsube et al., work in progress, 2006), such as storage porosity (ϕ_s) and connecting porosity (ϕ_c). These data will also be used for determining seal quality and other seal characteristics in future studies. This study documents the relationship between pore-size distribution and depth range with respect to four previously published compaction zones (Issler, 1992; Katsube and Issler, 1993) for the 41 shale samples. Trends in the porosity and density values are also investigated.

SAMPLE-COMPACTION ZONES

The 41 shale core samples were collected from Cretaceous and Paleocene sedimentary rocks over a depth range of approximately 950 to 4860 m in nine Beaufort-Mackenzie wells (Table 1; Katsube and Issler, 1993). The samples are from normally pressured, variably undercompacted and overpressured sedimentary rocks in four shale-compaction zones (Fig. 1; Issler, 1992). Late Pliocene to

Pleistocene (Iperk sequence) sedimentation rates vary from 570 to >1140 m/Ma, from 280 to 570 m/Ma, and from 50 to 280 m/Ma for zones 1 (Arluk E-90 and Nerlerk J-67 wells), 2 (Amauligak F-24 and Amerk O-09 wells), and 3 (Taglu wells), respectively (Issler et al., 2002). Zone 4 is characterized by differential exhumation (pre-Iperk sequence), which varies from approximately 500 m at the Mallik A-06 well to 800 m at the Reindeer D-27 well (Fig 1). Overpressure occurs below 2.3 km (main overpressure zone below 3 km) at Mallik A-06 and below approximately 2 km at Reindeer D-27 (Issler et al., 2002). Further details on the regional stratigraphy can be found in Issler (1992) and Issler et al. (2002).

EXPERIMENTAL RESULTS

Data on pore-size distribution for the 41 shale samples are listed in Tables 2 to 5 and shown graphically in Appendix A. They include data previously published and in the process of publication (Katsube and Issler, 1993; Issler and Katsube, 1994, Katsube et al., work in progress, 2006) on bulk and skeletal density (δ_{BD}, δ_{SD}), main pore-size-distribution mode (d_m), total porosity for the pore-size ranges of 0.03 to 10 µm and 0.03 to 250 µm (ϕ_{Hg1}, ϕ_{Hg2}), and geometric mean of the entire pore-size distribution (d_{Hg}). The parameter definitions are given in Table 2. The average values and standard deviations of these parameters for each of the four zones are listed in Table 6. The ranges of values for ϕ_{Hg1}, ϕ_{Hg2}, d_{Hg}, δ_{BD}, and δ_{SD} are 5.8 to 31.5%, 5.4 to 31.6%, 9.12 to 257 nm, 1.73 to 2.61 g/mL, and 2.26 to 2.82 g/mL, respectively. These values are plotted against depth (h) in Figure 2 for the four zones, and the δ_{BD}-h relationships for all 41 samples are shown in Figure 3. The values for ϕ_s and ϕ_c are in the range 2.0 to 17.3% and 1.6 to 18.9%, respectively. Methods for determining these parameters are described in previous publications (e.g. Katsube, 2000). The average pore-size distributions for the depth ranges <2 km and >2 km in each of the four compaction zones are shown in Figure 4. The average pore-size distributions for the samples from the overpressured and normally pressured areas of the four compaction zones are shown in Figure 5. The pore-size distributions for all 41 samples are grouped by zone in the appendix.

DISCUSSION AND CONCLUSIONS

The average pore-size distributions of the four zones (Fig. 4) show a distinct change at a depth of approximately 2 km, so a grouping was performed accordingly. This results in the two pore-size distributions for each of the four zones (Fig. 4). Little or no distinct change was noted in the pore-size distributions of samples from the normally pressured and overpressured areas of the four zones (Fig. 5). Although the differences between depths of >2 km and <2 km are obvious on Figure 4, they are less clear on Figure 2, particularly for δ_{BD} and δ_{SD}.

At shallower depths (<2 km), the main modes (d_{Hg}) are the intermediate pore sizes (10–1000 nm; Fig. 4a). In general, the partial porosities (ϕ_a) tend to decrease from zone 2 to zone 4 (Fig. 4a). This trend is represented by the decrease of the average total porosity values, ϕ_{Hg1} and ϕ_{Hg2}, from 28.5 to 16.1% and from 30.3 to 17.1%, respectively, for these two zones (Table 6). There are no data for zone 1 at the <2 km depth range.

At depths of >2 km (Fig. 4b), there is a general decrease in ϕ_a from zone 1 to zone 4, represented by the decrease of the average ϕ_{Hg1} and ϕ_{Hg2} values from 14.6 to 7.1% and from 15.8 to 7.5%, respectively (Table 6). The pore-size distributions are generally unimodal and asymmetric at this depth range. There tends to be a shift of the main mode from the intermediate pore sizes (25 nm to 10 µm) in zone 1 to the nano pore sizes (2.5–25 nm) in zone 4. The main difference in the pore-size distributions for the zones at this depth (>2 km) and those at shallower depths (<2 km) occurs in the intermediate and micro pore sizes (10–250 µm).

Some interesting trends are noted when comparing the ϕ_{Hg}-h and d_{Hg}-h relationships (Fig. 2). In this case, ϕ_{Hg} represents both ϕ_{Hg1} and ϕ_{Hg2}. Generally, they appear to follow a similar trend with increasing depth (i.e. as ϕ_{Hg} decreases, so does d_{Hg}). There are a few cases where d_{Hg} peaks and ϕ_{Hg} does not, such as in the 1 to 2 km depth range for zone 2 and in the 3 to 3.5 km depth range for zone 4. In zone 4, there is an abrupt decrease of both parameters in the <2 km depth range, followed by a levelling off until about the 3 km depth. At this point, ϕ_{Hg} decreases and d_{Hg} increases with depth. By 3.5 km, ϕ_{Hg} increases and d_{Hg} decreases again. There are only these few cases where the two values show opposite trends. The question that remains is whether these unusual trends have any significance, or whether they relate to lithological or structural changes.

In general, the δ_{BD} values increase with increasing depth (Fig. 3). There is a tendency for the δ_{BD} values and the gradient of the δ_{BD}-h relationship to increase from zone 1 to zone 4, except for the δ_{BD} values in the 2 to 4 km depth range of zone 4. In general, there is little to no difference in the δ_{BD} values or δ_{BD}-h relationships between the normally pressured and overpressured samples, except in the 2 to 4 km depth range of zone 4, where the δ_{BD}-h relationship tends to level off. The general increase in δ_{BD} values seen at individual depths and the increased δ_{BD}-h gradients from zone 1 to zone 4 may reflect the degree of compaction, with zone 1 still in the sedimentation stage and zone 4 in the stage of uplift from greater depth (Issler, 1992). The skeletal density or grain density (δ_{SD}) values of these 41 samples are in the range 2.63 to 2.78 g/mL (Table 6) and show little to no variation among the four zones, the depth ranges, or normally pressured and overpressured areas, as would be expected.

Table 2. Pore-size distribution for different pore-size ranges (d), obtained by mercury porosimetry, for five shale samples from zone 1 (Issler, 1992) of the Beaufort-Mackenzie Basin offshore, Northwest Territories.

Sample		NR-1	NR-2	NR-3	AK-1	AK-2
d (nm)	d_a (nm)	ϕ_a (%)				
2.5 - 4.0	3.2	1.01	0.77	0.60	1.08	1.80
4.0 - 6.3	5	0.71	0.82	0.72	0.98	1.32
6.3 - 10	7.9	0.90	1.00	0.97	1.08	1.80
10 - 16	12.6	0.81	1.02	0.93	1.10	2.01
16 - 25	20	1.34	2.00	1.76	2.20	3.57
25 - 40	31.6	1.96	4.21	2.71	2.90	0.77
40 - 63	50.1	4.15	4.33	2.99	1.39	0.43
63 - 100	79.4	3.39	0.39	0.77	0.65	0.31
100 - 160	126	0.46	0.18	0.26	0.36	0.24
160 - 250	200	0.28	0.23	0.23	0.31	0.14
250 - 400	316	0.12	0.14	0.12	0.14	0.14
400 - 630	501	0.14	0.16	0.12	0.22	0.14
630 - 1000	794	0.28	0.25	0.28	0.14	0.17
1000 - 1600	1259	0.18	0.14	0.21	0.02	0.14
1600 - 2500	1995	0.12	0.23	0.42	0.00	0.26
2500 - 4000	3162	0.02	0.16	0.42	0.00	0.24
4000 - 6300	5012	0.00	0.05	0.21	0.00	0.14
6300 - 10000	7943	0.09	0.11	0.30	0.07	0.38
ϕ_{Hg1}		15.90	16.20	14.00	12.70	14.00
ϕ_{Hg2}		16.90	16.70	15.40	13.10	16.80
d_{hg}		56.20	42.70	85.10	33.10	77.60
δ_{BD}		2.30	2.28	2.32	2.40	2.40
δ_{SD}		2.77	2.73	2.74	2.76	2.88
h		3.66	3.67	4.01	3.45	3.94
ϕ_s		7.10	7.60	8.30	6.40	9.20
ϕ_c		8.80	8.60	5.70	6.40	4.80
ϕ_{rr}		0.45	0.47	0.59	0.50	0.66

d = Pore-size range (nm)
d_a = Geometric mean pore sizes for the different pore-size ranges (nm)
d_{hg} = Geometric mean of the entire pore-size distribution (nm)
ϕ_a = Partial porosity (%), representing the porosity for specific pore-size ranges (d)
ϕ_{Hg1} = Total porosity, measured by mercury porosimetry, for pore sizes from 2.5 nm to 10 µm (%)
ϕ_{Hg2} = Total porosity, measured by mercury porosimetry, for pore sizes from 2.5 nm to 250 µm (%)
δ_{BD} = Bulk density (g/mL)
δ_{SD} = Skeletal or grain density (g/mL)
h = True vertical depth (TVD, km)
ϕ_s = Storage porosity (%)
ϕ_c = Connecting porosity (%)
ϕ_{rr} = Storage porosity ratio ($\phi_S/(\phi_S+\phi_C)$)

Table 3. Pore-size distribution for different pore-size ranges (d), obtained by mercury porosimetry, for 10 shale samples from zone 2 of the Beaufort-Mackenzie Basin offshore, Northwest Territories.

	AM-1	AM-2	AM-3	AR-1	AR-2	AR-3	AR-4	AR-5	AR-6	AR-7
d_a (nm)	ϕ_a (%)									
1.26	0.00	0.00	0.00	0.00	0.00	0.00	0.00	0.00	0.00	0.00
2	0.00	0.00	0.00	0.00	0.00	0.00	0.00	0.00	0.00	0.00
3.2	0.73	1.25	0.73	0.61	1.31	0.02	1.02	0.81	1.00	0.60
5	0.78	1.01	0.71	0.76	1.19	0.29	0.90	0.84	0.98	0.90
7.9	1.05	1.30	0.95	1.09	0.93	1.11	1.22	1.41	1.45	1.32
12.6	0.95	1.27	0.85	1.01	0.64	0.96	1.36	2.42	2.20	2.87
20	1.45	2.81	1.53	1.44	0.78	1.53	1.46	1.13	1.53	1.32
31.6	1.45	1.66	1.73	1.59	0.84	1.66	0.66	0.25	0.28	0.25
50.1	1.53	0.41	1.46	2.74	1.27	2.62	0.63	0.20	0.28	0.25
79.4	0.60	0.22	0.46	5.44	2.03	3.67	0.46	0.10	0.18	0.12
126	0.20	0.14	0.17	5.93	2.15	3.16	0.36	0.12	0.13	0.12
200	0.15	0.12	0.15	5.48	2.76	3.75	0.53	0.10	0.13	0.10
316	0.08	0.02	0.02	0.97	1.65	1.93	0.27	0.07	0.00	0.00
501	0.08	0.07	0.12	0.99	2.19	2.75	0.66	0.12	0.05	0.07
794	0.08	0.07	0.15	0.73	2.70	2.09	0.39	0.20	0.05	0.07
1259	0.05	0.07	0.07	0.36	1.69	0.87	0.07	0.10	0.03	0.05
1995	0.50	0.14	0.07	0.38	1.65	0.87	0.10	0.17	0.00	0.00
3162	0.00	0.07	0.10	0.33	1.27	0.55	0.10	0.17	0.00	0.02
5012	0.00	0.10	0.02	0.50	0.04	0.23	0.00	0.10	0.00	0.00
7943	0.10	0.10	0.10	1.13	0.72	0.23	0.12	0.15	0.10	0.07
ϕ_{Hg1}	9.80	10.80	9.40	31.50	25.80	28.30	10.30	8.50	8.40	8.20
ϕ_{Hg2}	10.00	12.00	10.10	31.60	29.20	30.00	11.50	9.60	8.80	8.60
d_{hg}	47.90	38.00	43.70	117.00	331.00	200.00	70.80	47.90	20.90	21.40
δ_{BD}	2.50	2.40	2.44	1.73	1.99	1.78	2.43	2.47	2.50	2.50
δ_{SD}	2.78	2.73	2.71	2.54	2.81	2.55	2.75	2.73	2.74	2.73
h	3.11	3.12	3.34	1.32	1.53	1.77	3.87	4.38	4.61	4.86
ϕ_s	5.40	5.80	4.90	12.50	17.30	15.70	6.10	6.20	4.60	4.80
ϕ_c	4.40	5.00	4.50	18.90	8.50	12.50	4.10	2.30	3.80	3.40
ϕ_{rr}	0.55	0.54	0.52	0.40	0.67	0.56	0.60	0.73	0.55	0.59

d = Pore-size range (nm). See column 1 in Table 2
d_a = Geometric mean pore sizes for the different pore-size ranges (nm)
d_{hg} = Geometric mean of the entire pore-size distribution (nm)
ϕ_a = Partial porosity (%), representing the porosity for specific pore-size ranges (d)
ϕ_{Hg1} = Total porosity, measured by mercury porosimetry, for pore sizes from 2.5 nm to 10 µm (%)
ϕ_{Hg2} = Total porosity, measured by mercury porosimetry, for pore sizes from 2.5 nm to 250 µm (%)
δ_{BD} = Bulk density (g/mL)
δ_{SD} = Skeletal or grain density (g/mL)
h = True vertical depth (TVD, km)
ϕ_s = Storage porosity (%)
ϕ_c = Connecting porosity (%)
ϕ_{rr} = Storage porosity ratio ($\phi_S/(\phi_S+\phi_C)$)

Table 4. Pore-size distribution for different pore-size ranges (d), obtained by mercury porosimetry, for nine shale samples from zone 3 of the Beaufort-Mackenzie Basin offshore, Northwest Territories.

	TG-1	TG-2	TG-3	TG-4	TG-5	TG-6	TG-7	TA-1	TA-2
d_a	ϕ_a (%)								
3.2	1.16	0.66	0.91	1.17	1.38	0.89	0.69	2.00	0.90
5	0.82	0.79	1.09	1.21	1.35	1.33	0.79	1.45	0.92
7.9	0.90	0.87	1.25	1.33	1.78	1.61	1.06	1.11	1.20
12.6	0.66	0.75	1.32	1.52	0.87	0.97	1.03	0.53	1.48
20	0.92	1.06	2.94	3.57	0.69	0.66	1.99	0.44	1.77
31.6	0.86	1.20	6.24	2.12	0.31	0.28	1.06	0.19	0.72
50.1	1.24	2.24	3.71	0.67	0.25	0.26	1.15	0.17	0.28
79.4	1.80	3.92	0.59	0.36	0.15	0.18	0.79	0.11	0.13
126	1.95	3.86	0.14	0.12	0.13	0.10	0.44	0.08	0.10
200	3.22	3.77	0.09	0.21	0.13	0.13	0.42	0.06	0.08
316	2.58	0.79	0.09	0.10	0.05	0.05	0.12	0.00	0.00
501	5.32	0.66	0.02	0.05	0.08	0.05	0.07	0.00	0.00
794	5.79	0.68	0.02	0.12	0.13	0.13	0.10	0.00	0.00
1259	0.94	0.35	0.00	0.00	0.03	0.05	0.05	0.00	0.00
1995	0.73	0.54	0.00	0.00	0.08	0.08	0.10	0.00	0.00
3162	0.36	0.39	0.00	0.00	0.03	0.08	0.02	0.00	0.00
5012	0.11	0.21	0.00	0.00	0.00	0.03	0.00	0.00	0.00
7943	0.19	0.08	0.18	0.05	0.13	0.05	0.07	0.15	0.08
ϕ_{Hg1}	29.50	22.80	18.60	12.60	7.60	6.90	10.00	6.30	7.70
ϕ_{Hg2}	30.60	23.50	19.20	14.20	8.30	7.80	10.70	7.00	8.00
d_{hg}	229.00	115.00	31.60	26.30	28.20	36.30	44.70	20.40	20.90
δ_{BD}	1.87	2.07	2.28	2.38	2.46	2.55	2.46	2.10	2.56
δ_{SD}	2.70	2.71	2.82	2.74	2.78	2.77	2.75	2.26	2.78
h	0.95	1.35	1.64	2.08	2.46	2.46	2.53	2.88	3.25
ϕ_s	16.20	13.90	8.40	6.70	5.20	5.30	5.90	2.00	4.10
ϕ_c	13.30	8.90	10.20	5.90	2.40	1.60	4.10	4.30	3.50
ϕ_{rr}	0.55	0.61	0.45	0.53	0.69	0.77	0.59	0.32	0.54

d = Pore-size range (nm). See column 1 in Table 2.
d_a = Geometric mean pore sizes for the different pore-size ranges (nm)
d_{hg} = Geometric mean of the entire pore-size distribution (nm)
ϕ_a = Partial porosity (%), representing the porosity for specific pore-size ranges (d)
ϕ_{Hg1} = Total porosity, measured by mercury porosimetry, for pore sizes from 2.5 nm to 10 µm (%)
ϕ_{Hg2} = Total porosity, measured by mercury porosimetry, for pore sizes from 2.5 nm to 250 µm (%)
δ_{BD} = Bulk density (g/mL)
δ_{SD} = Skeletal or grain density (g/mL)
h = True vertical depth (TVD, km)
ϕ_s = Storage porosity (%)
ϕ_c = Connecting porosity (%)
ϕ_{rr} = Storage porosity ratio ($\phi_S/(\phi_S+\phi_C)$)

Table 5. Pore-size distribution for different pore-size ranges (d), obtained by mercury porosimetry, for 17 shale samples from zone 4 of the Beaufort-Mackenzie Basin offshore, Northwest Territories.

	ML-1	ML-2	ML-3	RE-1	RE-2	RE-3	RE-4	RE-5	RE-6	RE-7	RE-8	RE-9	RE-10	RE-11	RE-12	RE-13	RE-14
d_a	ϕ_a (%)																
3.2	0.14	0.26	1.15	0.68	0.89	1.21	1.85	0.91	1.05	0.82	0.67	0.84	0.72	0.86	0.73	1.63	1.42
5	0.21	0.44	1.10	0.80	0.98	1.26	1.38	1.01	0.92	0.92	0.77	0.87	0.87	1.40	0.94	1.45	1.83
7.9	0.80	0.63	1.31	1.05	1.08	1.59	1.62	1.70	1.48	1.42	1.07	1.48	1.39	2.46	1.97	1.25	2.19
12.6	0.78	0.73	1.02	0.84	1.01	1.00	1.04	1.29	1.33	2.17	1.34	2.79	2.33	2.24	1.52	0.38	0.39
20	1.21	1.41	0.55	1.38	1.90	0.39	0.47	0.53	0.84	2.20	2.23	1.81	2.63	0.69	0.41	0.31	0.28
31.6	1.23	0.89	0.21	1.19	1.41	0.15	0.26	0.20	0.28	0.42	0.89	0.30	0.42	0.25	0.23	0.18	0.21
50.1	1.66	0.42	0.21	1.45	0.94	0.13	0.18	0.15	0.20	0.25	0.35	0.20	0.22	0.17	0.15	0.18	0.15
79.4	1.93	0.13	0.10	1.41	0.82	0.05	0.18	0.13	0.15	0.15	0.17	0.12	0.12	0.10	0.10	0.13	0.13
126	1.62	0.05	0.05	1.01	0.56	0.05	0.03	0.08	0.08	0.10	0.07	0.07	0.12	0.12	0.08	0.03	0.08
200	2.23	0.03	0.00	1.17	0.63	0.03	0.00	0.05	0.08	0.07	0.07	0.07	0.10	0.02	0.08	0.00	0.08
316	1.41	0.00	0.00	0.68	0.33	0.03	0.00	0.05	0.03	0.02	0.02	0.05	0.02	0.05	0.03	0.00	0.05
501	2.01	0.03	0.00	1.34	0.54	0.00	0.00	0.03	0.03	0.02	0.07	0.02	0.10	0.05	0.05	0.00	0.05
794	3.24	0.05	0.00	1.31	0.66	0.00	0.00	0.03	0.00	0.00	0.05	0.07	0.05	0.00	0.10	0.00	0.08
1259	1.23	0.00	0.00	0.30	0.16	0.00	0.00	0.00	0.00	0.00	0.05	0.02	0.05	0.00	0.05	0.00	0.03
1995	0.86	0.03	0.00	0.19	0.12	0.00	0.00	0.00	0.00	0.00	0.00	0.07	0.02	0.00	0.05	0.00	0.00
3162	0.31	0.00	0.00	0.00	0.00	0.00	0.00	0.00	0.00	0.00	0.00	0.00	0.02	0.00	0.05	0.00	0.00
5012	0.14	0.00	0.00	0.00	0.00	0.00	0.00	0.00	0.00	0.00	0.00	0.02	0.00	0.00	0.00	0.00	0.00
7943	0.25	0.00	0.10	0.14	0.07	0.03	0.03	0.08	0.10	0.07	0.10	0.07	0.05	0.05	0.08	0.05	0.08
ϕ_{Hg1}	21.30	5.10	5.80	15.00	12.10	5.90	7.00	6.20	6.60	8.70	7.90	8.90	9.30	8.50	6.60	5.60	7.00
ϕ_{Hg2}	22.90	5.40	6.40	15.50	12.80	6.70	7.60	6.70	7.00	9.10	8.50	9.40	9.50	8.90	7.10	5.70	7.40
d_{hg}	257.00	32.30	19.40	95.50	51.30	19.50	14.50	20.00	20.40	19.50	26.30	20.90	20.00	16.20	24.00	9.12	14.10
δ_{BD}	2.05	2.61	2.61	2.34	2.34	2.57	2.61	2.53	2.56	2.50	2.48	2.47	2.48	2.46	2.53	2.55	2.58
δ_{SD}	2.66	2.76	2.79	2.77	2.69	2.75	2.82	2.71	2.75	2.74	2.71	2.73	2.74	2.70	2.73	2.70	2.79
h	1.36	3.18	3.55	1.46	1.47	2.02	2.09	2.10	2.21	2.39	2.42	2.55	2.73	2.92	3.15	3.48	3.63
ϕ_s	14.40	3.20	3.30	9.10	7.00	3.40	2.70	3.50	3.60	4.60	4.20	5.10	5.10	4.70	4.10	2.60	4.00
ϕ_c	7.00	1.80	2.50	6.00	5.20	2.50	4.30	2.70	3.00	4.10	3.70	3.80	4.20	3.80	2.60	3.00	3.00
ϕ_{rr}	0.67	0.64	0.57	0.60	0.57	0.58	0.38	0.56	0.54	0.53	0.53	0.57	0.55	0.55	0.61	0.46	0.57

See Table 4 for explanation of abbreviations.

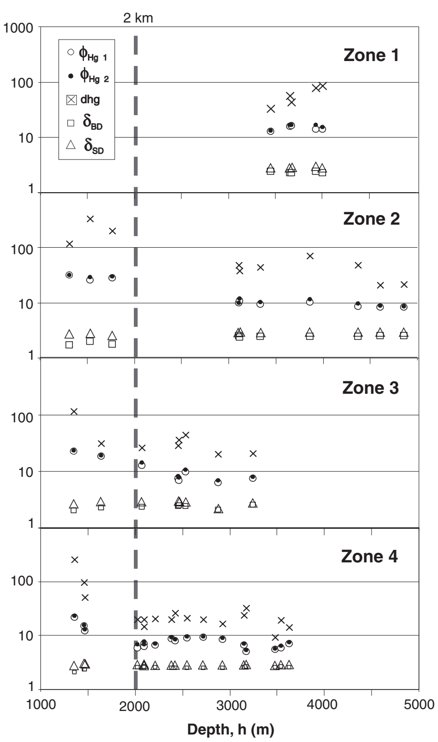

Figure 2. Plots of total porosity for the 2.5 nm to 10 µm pore-size range (ϕ_{Hg1}), total porosity for the 2.5 nm to 250 µm pore-size range (ϕ_{Hg2}), geometric mean of the entire pore-size distribution (d_{Hg}), bulk density (δ_{BD}), and skeletal or grain density (δ_{SD}) versus depth (h) for zones 1 through 4, Beaufort-Mackenzie Basin offshore, Northwest Territories.

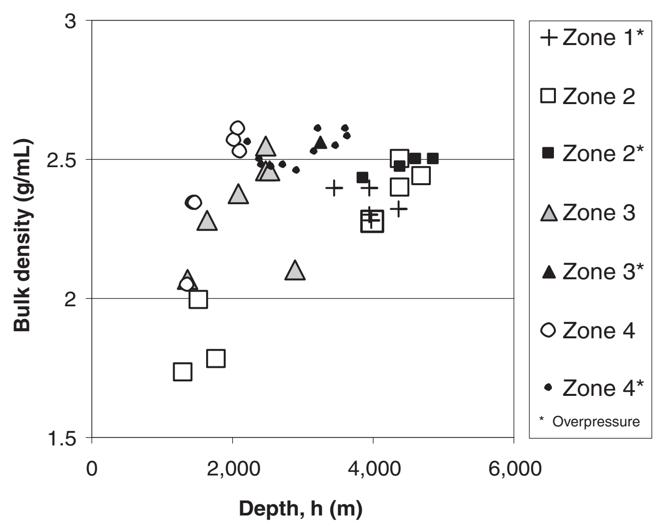

Figure 3. Plot of bulk density (δ_{BD}) versus depth (h) for each of the four zones, Beaufort-Mackenzie Basin offshore, Northwest Territories. Samples from the overpressured and normally pressured zones are also identified

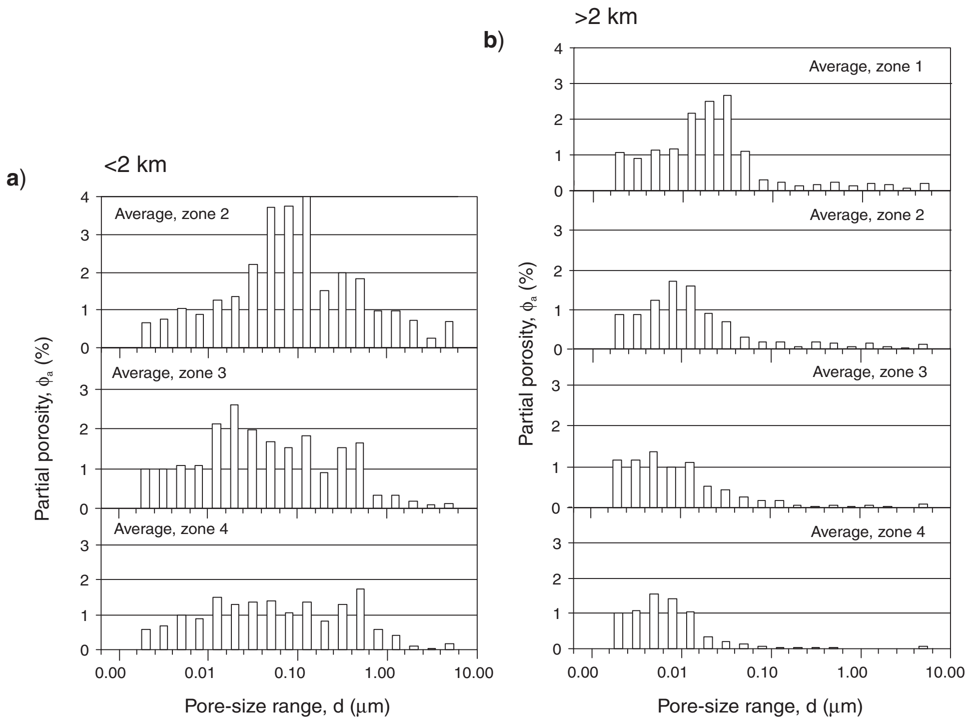

Figure 4. Average pore-size distributions for zones 1 through 4, Beaufort-Mackenzie Basin offshore, Northwest Territories: **a)** <2 km depth range, and **b)** >2 km depth range.

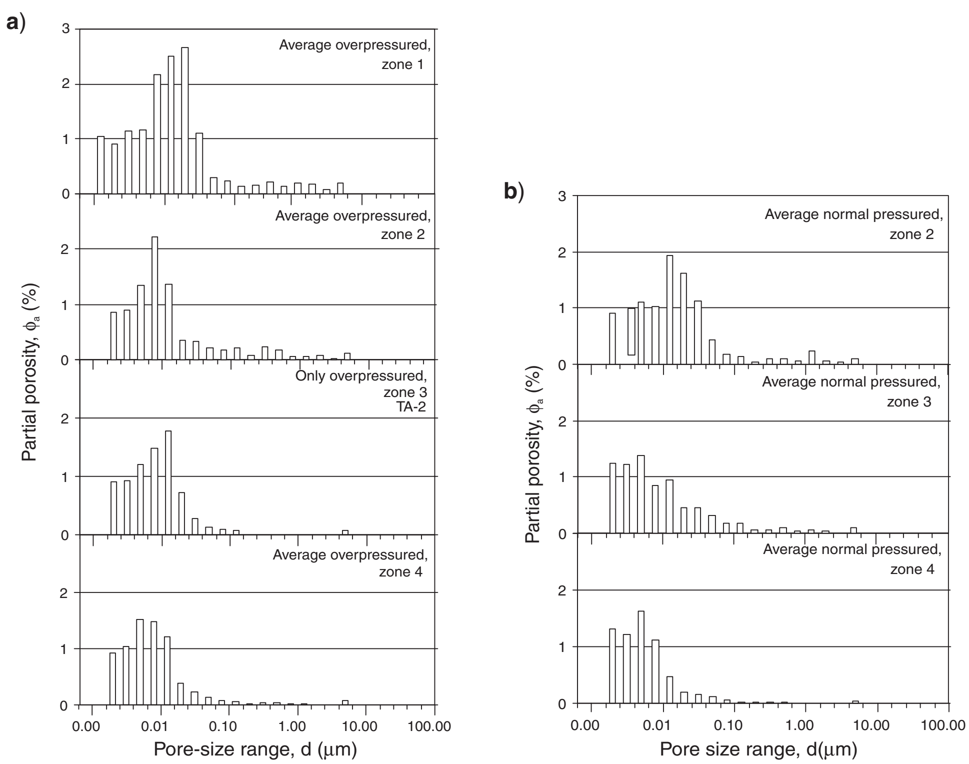

Figure 5. Average pore-size distributions for zones 1 through 4, Beaufort-Mackenzie Basin offshore, Northwest Territories: **a)** overpressured samples, and **b)** normally pressured samples.

Table 6. Average values for ϕ_{Hg1}, ϕ_{Hg2}, d_{hg}, δ_{BD}, and δ_{SD} for depth ranges of <2 km and >2 km in zones 1, 2, 3, and 4, Beaufort-Mackenzie Basin offshore, Northwest Territories.

Zone	ϕ_{Hg1}		ϕ_{Hg2}		dhg		δ_{BD}		δ_{SD}	
	<2 km	**>2 km**	**<2 km**	**>2 km**	**<2 km**	**>2 km**	**<2 km**	**>2 km**	**<2 km**	**>2 km**
1	n/a	14.56 ± *1.46*	n/a	15.78 ± 1.62	n/a	58.94 ± 22.2	n/a	2.34 ± 0.0	n/a	2.78 ± 0.06
2	28.53 ± 2.86	9.32 ± 1.03	30.27 ± 1.22	10.09 ± 1.28	216 ± 107.89	41.51 ± 17.25	1.83 ± 0.14	2.46 ± 0.04	2.63 ± 0.15	2.74 ± 0.02
3	20.7 ± 2.97	8.49 ± 2.36	21.35 ± 3.04	9.33 ± 2.69	73.3 ± 58.97	29.47 ± 9.44	2.175 ± 0.15	2.42 ± 0.17	2.765 ± 0.08	2.68 ± 0.21
4	16.13 ± 4.7	7.08 ± 1.35	17.07 ± 5.23	7.53 ± 1.35	134.60 ± 108.3	19.73 ± 5.59	2.24 ± 0.17	2.54 ± 0.05	2.71 ± 0.06	2.74 ± 0.04

See Table 4 for explanation of abbreviations.

ACKNOWLEDGMENTS

The authors thank B. Medioli (Geological Survey of Canada – Ottawa) for critically reviewing this paper and for her constructive suggestions. The authors also thank D. Issler (Geological Survey of Canada – Calgary) for his very constructive comments and suggestions. The authors acknowledge the efficient work carried out by B. Smith (ORTECH International, Toronto, Ontario) on the mercury porosimetry measurements.

REFERENCES

Huffman, A.R. and Bowers, G.L. (ed.)
2002: Pressure regimes in sedimentary basins and their prediction; American Association of Petroleum Geologists, Memoir 76, 237 p.

Issler, D.R.
1992: A new approach to shale compaction and stratigraphic restoration, Beaufort-Mackenzie Basin and Mackenzie corridor, northern Canada; American Association of Petroleum Geologists Bulletin, v. 76, p. 1170–1189.

Issler, D.R. and Katsube, T.J.
1994: Effective porosity of shale samples from the Beaufort-Mackenzie Basin; *in* Current Research, Part B; Geological Survey of Canada, Paper 94-1B, p. 19–26.

Issler, D.R., Katsube, T.J., Bloch. J.D., and McNeil, D.H.
2002: Shale compaction and overpressure in the Beaufort-Mackenzie Basin of northern Canada; Geological Survey of Canada, Open File 4192, CD-ROM.

Katsube, T.J.
2000: Shale permeability and pore-structure evolution characteristics: implications for overpressure; Geological Survey of Canada, Current Research 2000-E15, 9 p.

Katsube, T.J. and Connell, S.
1998: Shale permeability characteristics; *in* Current Research 1998-E; Geological Survey of Canada, p. 183–192.

Katsube, T.J. and Issler, D.R.
1993: Pore-size distribution of shales from the Beaufort-Mackenzie Basin, northern Canada; *in* Current Research, Part E; Geological Survey of Canada, Paper 93-1E, p. 123–132.

Katsube, T.J. and Jonasson, I.R
2002: Possible seal mechanisms in shallow sediments: implications for shallow-water flow; Society of Exploration Geophysicists Summer Research Workshop, May 12–17, 2002, Galveston, Texas, Presentations and Abstracts, Session II, abstract, summary and 12 slides.

Katsube, T.J. and Williamson, M.A.
1998: Shale petrophysical characteristics: permeability history of subsiding shales; *in* Shales and Mudstones II: Petrography, Petrophysics, Geochemistry and Economic Geology, (ed.) J. Schieber, W. Zimmerle, and P.S. Sethi; E. Schweizerbart Science Publishers, Stuttgart, Germany, p. 69–91.

Katsube, T.J., Dallimore, S.R., Uchida, T., Jenner, K.A., Collett, T.S., and Connell, S.
1999: Petrophysical environment of sediments hosting gas hydrate, JAPEX/JNOC/GSC Mallik 2L-38 gas hydrate research well; *in* Scientific Results from JAPEX/JNOC/GSC Mallik 2L-38 Gas Hydrate Research Well, Mackenzie Delta, Northwest Territories, Canada, (ed.) S.R. Dallimore, T. Uchida, and T.S. Collett; Geological Survey of Canada, Bulletin 544, p. 109–124.

Katsube, T.J., Jonasson, I.R., Uchida, T., and Connell-Madore, S.
2004: Possible seal mechanisms in shallow sediments and their implication for gas-hydrate accumulation; *in* Gas Hydrates: Energy Resource Potential and Associated Geologic Hazards, (ed.) T. Collett and A. Johnson; American Association of Petroleum Geologists, Proceedings of Hedberg Conference, September 12–16, 2004, Vancouver, British Columbia, abstract, 4 p.

Geological Survey of Canada Project Y08

APPENDIX A

Pore size distribution plots for all shale samples from the Beaufort-Mackenzie Basin, Northwest Territories

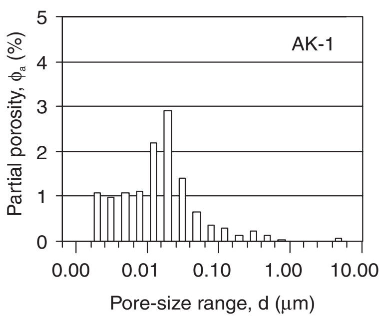

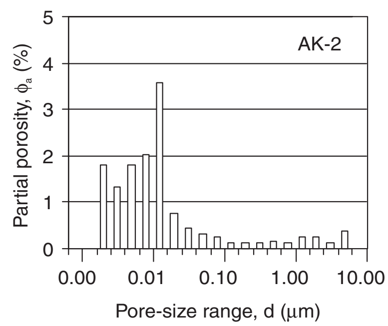

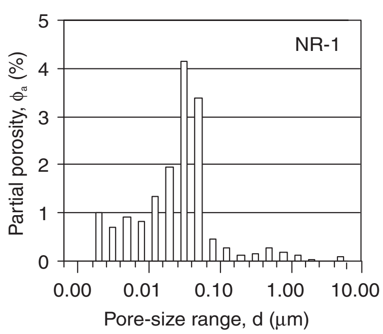

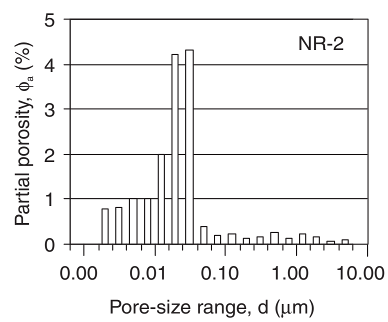

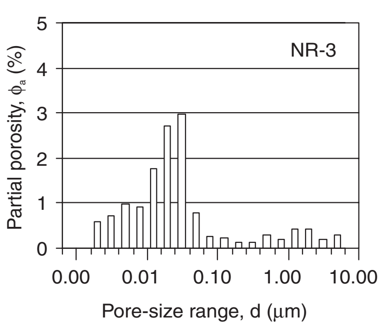

Appendix A (cont.)

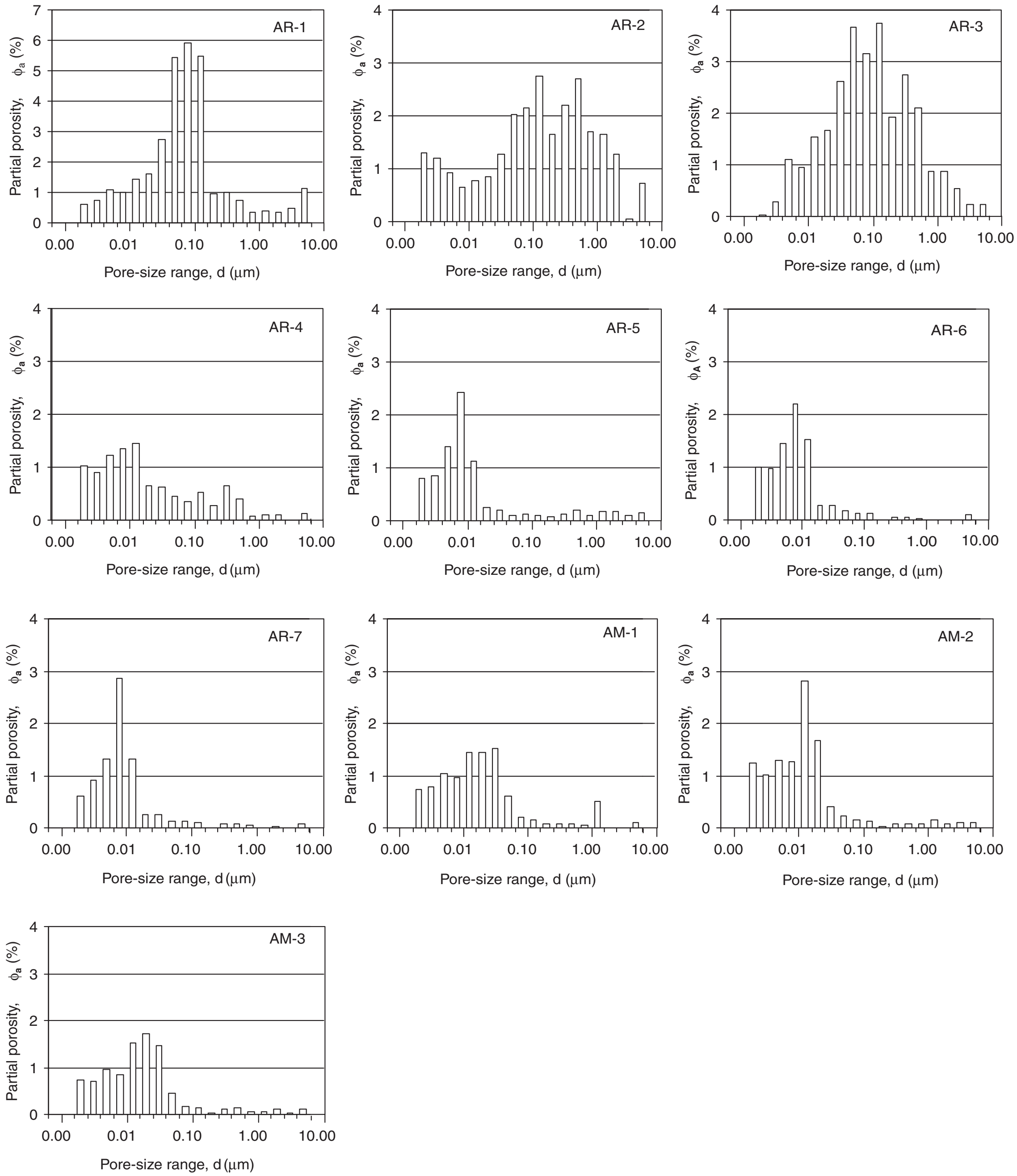

Appendix A (cont.)

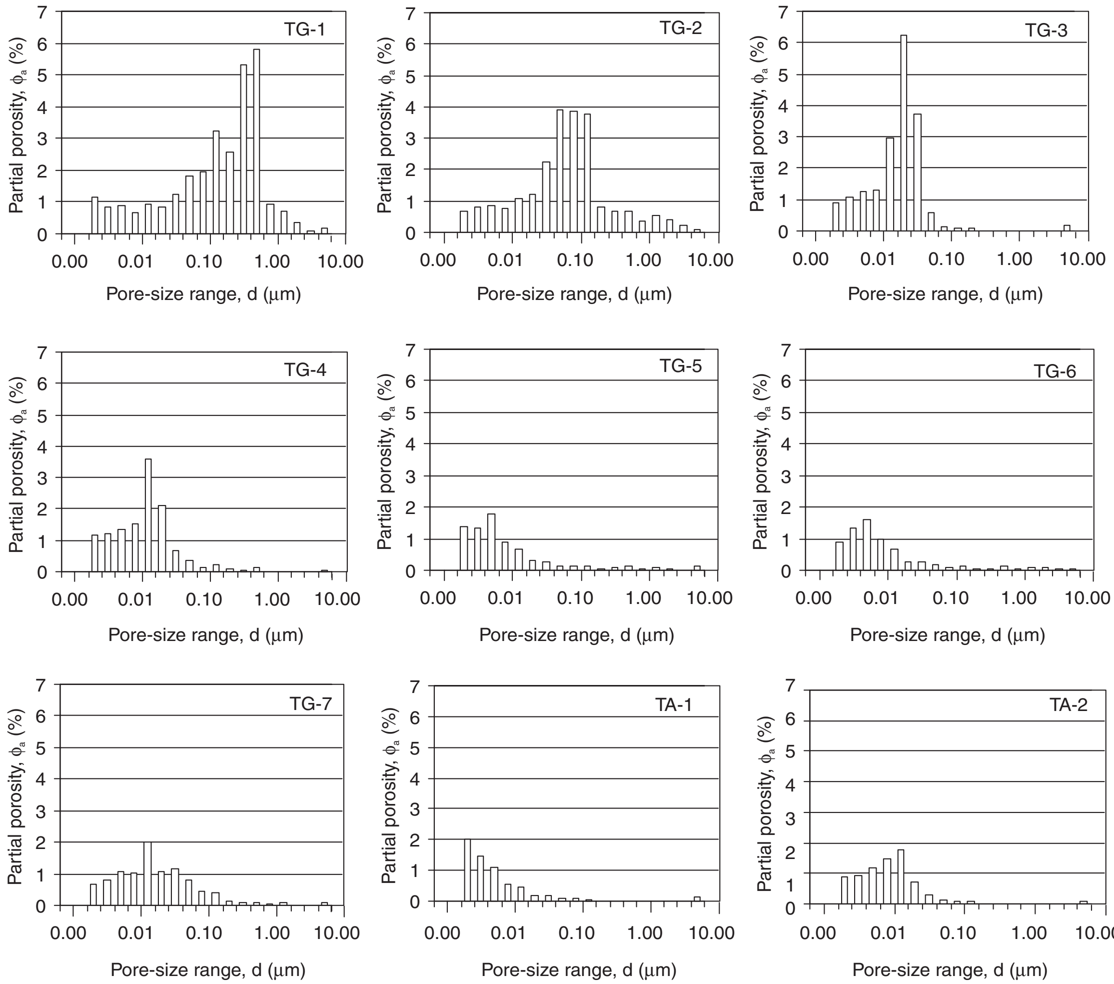

Appendix A (cont.)

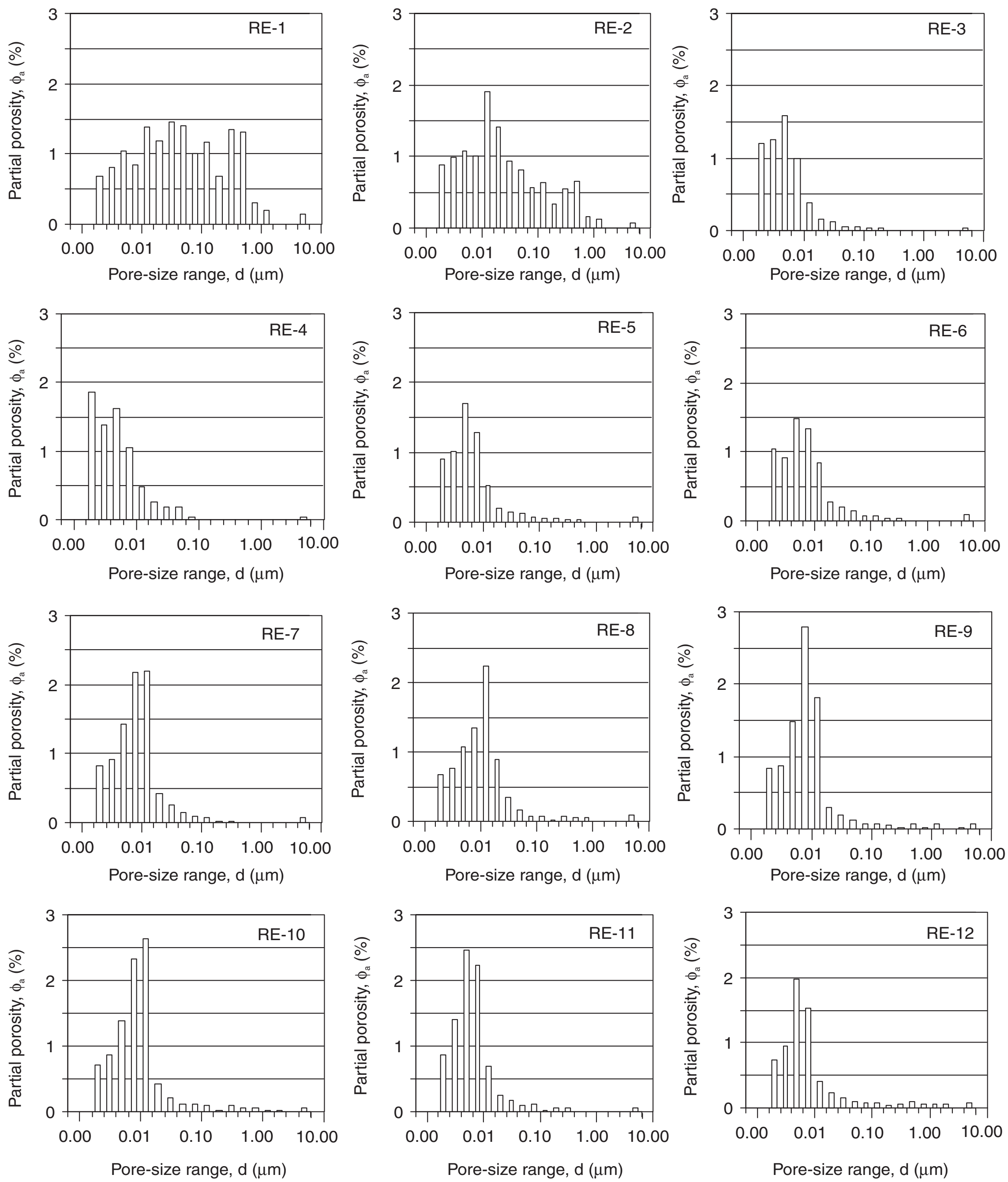

Appendix A (cont.)